Out-of-Plane Vibration Frequency Estimation for Flexible Substrate in Roll-to-Roll Processing

Jiankui Chen(✉), Yufei Zhu, Hua Yang, Yongan Huang, and Zhouping Yin

State Key Laboratory of Digital Manufacturing Equipment and Technology, Flexible Electronics Research Center, Huazhong University of Science and Technology, Wuhan 430074, China
chenjk@hust.edu.cn

Abstract. Out-of-plane displacements of a moving web is well known to be a main limiting factor of roll-to-roll (R2R) manufacturing for flexible electronics. To tackle this problem, in this paper, a new contactless approach for the measurement of membrane vibration is addressed. This technique, which allows catching out-of-plane membrane vibration involves a vision system composed of a CCD camera and a laser stripe device. With gray centroid method and principal component analysis, out-of-plane vibration distribution is estimated in real time. Experiments are conducted on the RFID inlay in R2R experimental platform to confirm the effectiveness and accuracy of the proposed method.

Keywords: Out-of-plane vibration · Flexible electronics · Roll-to-roll
Frequency estimation · Structured light

1 Introduction

Flexible electronics, also known as printed or organic electronics, are depositing organic/inorganic electronic devices on a flexible web [1]. Its production process can be integrated by roll-to-roll (R2R) manufacturing, and the main objective is to increase the web velocity while controlling the tension of the web. This can improve the production efficiency of flexible electronics. However, some disturbances limit the velocity, like the non-circularity of the roll, roll misalignment and web sliding, etc. What's more, since there exists a coupling introduced by the elastic property of the flexible web, disturbances are transmitted to the web tension, resulting in web out-of-plane vibrations. Therefore, the out-of-plane vibration measurement is meaningful for perceiving the web tension change and improving the production efficiency of flexible electronics.

The out-of-plane vibration can be measured by several methods in the R2R system. Traditionally, laser sensor set vertical to the web is used to measure out-of-plane displacements [2–4], which is fast and high-precise. However, this method is affected by the accuracy of laser sensors and can only achieve the vibration information of one point in the web surface. With the development of machine vision and image processing technology, vision-based measuring methods are used to measure vibration

Z. Chen et al. (Eds.): ICIRA 2018, LNAI 10984, pp. 331–341, 2018.
https://doi.org/10.1007/978-3-319-97586-3_30

gradually. Maurice [5] proposed a new framework for the design of patterns driven by the Hamming distance with coded structured light, and, the 3-D information can be obtained accurately. Ishii [6] investigated a high-frame-rate laryngoscope including a high-speed camera at 4000 fps to measure the vibration distribution of a human vocal fold. Zhai [7] studied a method by projecting π phase shifting bi-color sinusoidal fringe to analyze the vibration of membrane. Doignon [8] proposed a new technique to estimate out-of-plane web vibration properties with a camera and a laser dot pattern device and experiments was performed. Doignon [9] also presented a faster stereovision system in conjunction with a more appropriate laser stripe line pattern. This method can be used for non-contact measurement of the whole web surface.

In this paper, a measuring system composed of a CCD camera and a laser stripe device is built to measure the out-of-plane displacement of the horizontal moving web between two rolls. Firstly, with stripe structured light principle, the geometric model of vibration measurement system is built to get the relationship between the out-of-plane displacements of moving web and the coordinates of the laser stripe in the images. Then, gray centroid method is used to derive initial centerline coordinates of laser stripe. Principal component analysis is used to derive initial centerline normal vectors to get precise coordinates. Finally, coordinates are transformed into out-of-plane displacements and the natural frequencies are also calculated based on the Fourier transform. Experiments are carried out to confirm the proposed method.

2 Geometrical Model

The geometrical model of the whole vision system is briefly described in this section. To get actual coordinates of points in the web surface, the relationship between image plane coordinates and world coordinates is built. The stationary web plane is on the base plane $O_wX_wY_w$. The well-known pinhole camera model is used to relate a 3-D point P in the web surface, with homogeneous coordinates $(x^W, y^W, z^W, 1)^T$ expressed in the world coordinate system and its corresponding projection $(m, n, 1)^T$ in the image plane coordinate system. That is:

$$z^C \begin{bmatrix} m \\ n \\ 1 \end{bmatrix} = \begin{bmatrix} 1/m_x & 0 & 0 \\ 0 & 1/n_x & 0 \\ 0 & 0 & 1 \end{bmatrix} \begin{bmatrix} f & 0 & 0 & 0 \\ 0 & f & 0 & 0 \\ 0 & 0 & 1 & 0 \end{bmatrix} \begin{bmatrix} R & T \\ 0 & 1 \end{bmatrix} \begin{bmatrix} x^W \\ y^W \\ z^W \\ 1 \end{bmatrix} \tag{1}$$

where m_x, n_x are the sizes of CCD camera cells and f is focal length. Rotation matrix R and translation vector T are used to describe the conversion relation between world coordinate system and camera coordinate system.

Also, in order to get the out-of-plane displacements, the relationship between the displacements at any point of the projected stripe and the coordinates of the point in the image is established. The geometrical model of the web vibration measuring system is shown in Fig. 1. Based on the traditional 3-D measurement system of structured light, we optimize the system geometry and weaken the geometric constraints (see Fig. 1(a)). The optical axis of the camera is not intersected with the light axis of the laser device

on the base plane. The optical axis of the camera and the light axis of the laser device don't need to be perpendicular to the base plane. Also, the line of the camera optical center and laser optical center don't need to be parallel. In general, we assume that laser stripe projected on the base plane is not perpendicular to the Y^W axis. Instead, it is perpendicular to the auxiliary line L, and the angle between the line L and the X^W axis is θ (see Fig. 1(b)).

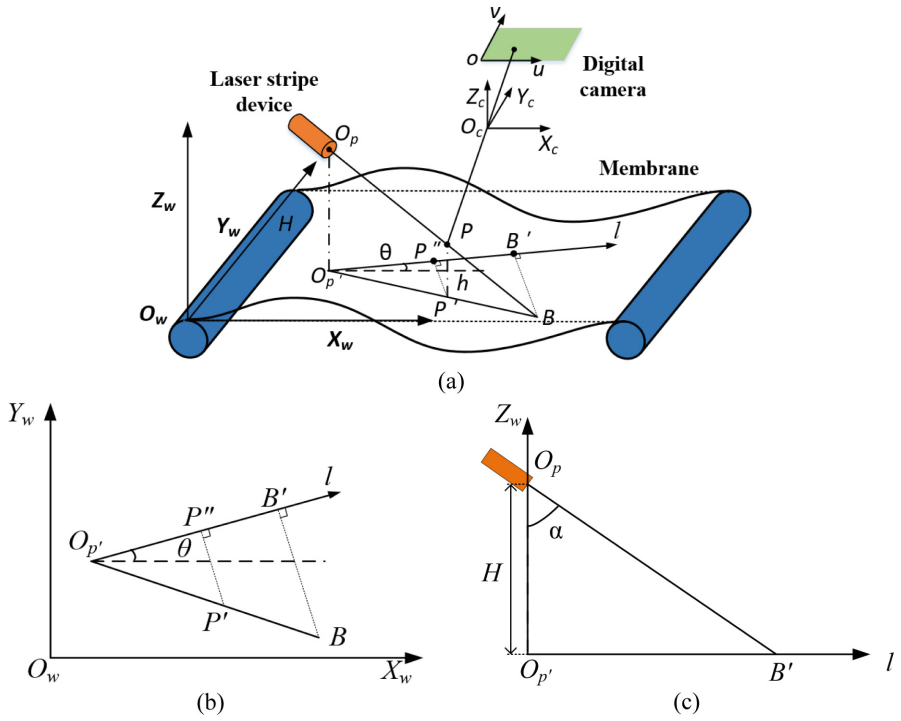

Fig. 1. The geometrical model of the web vibration measuring system (a) Optical path of measuring system; (b) Geometric distribution of base plane; (c) 2-D structure of projection system.

According to the similar triangle and geometric relationship, the formula between the world coordinates on the web surface and the vibration displacements of the point P can be established as follow:

$$h = H - \frac{(x^W - x_0)\cos\theta - (y^W - y_0)\sin\theta}{H\ \tan\alpha} \tag{2}$$

where H is the distance of laser optical center O_p to the base plane $O^W X^W Y^W$, $(x^W, y^W, 0)$ is the world coordinates of the projected point P' and $(x_0, y_0, 0)$ is the world coordinates of the projected point O'_p.

Finally, the approximate fitting formula of the web vibration measuring system model can be described as

$$h = (A_1 + A_2 m + A_3 n)/(B_1 + B_2 m + B_3 n) \tag{3}$$

where the coefficients A_1, A_2, A_3, B_1, B_2 and B_3 are dependent on the geometric parameters and camera intrinsic parameters.

Therefore, once the image plane coordinates of the points are obtained, the out-of-plane displacements can be computed from Eq. (3) immediately.

3 Theoretical Analysis

3.1 Out-of-Plane Vibration Equation

The equations of an axially moving a string or beam can be derived from the extended Hamilton principle and consist of two partial different equations [10]. A numerical study shows that, in our experimental conditions, the coupling in the longitudinal and out-of-plane vibrations through the web tension is not significant, and this was experimentally observed [11]. Therefore, these equations can be decoupled and simplified under the realistic assumption that the web velocity and tension remain constant. The equation is given as

$$(V^2 - \frac{T}{\rho})\frac{\partial^2 y}{\partial x^2} + 2V\frac{\partial^2 y}{\partial t \partial x} + \frac{\partial^2 y}{\partial t^2} = 0 \tag{4}$$

where y, ρ, V, T represent the out-of-plane displacement, the linear web density, the web speed and the web tension. So, the natural frequencies for a stationary web model without stiffness can be given as $f_1 = c/2L$, and the natural frequencies for a moving web model without stiffness can be given as $f_2 = c(1 - V^2/c^2)/2L$. The natural frequencies will be used to compare with the experimental results. It is important to emphasize that the proposed method in this paper is to measure the vibration distribution of the web surface and its working condition is different from the realistic condition of this string model. Therefore, the contrast can only be used as a general reference.

3.2 Centerline Extraction of Structured Light Strip

In this section, we propose a new method to estimate the accurate coordinates of the laser stripe centerline, which is based on principal component analysis (PCA). The measuring procedure includes grabbing the laser strip images, extracting the region of interest, computing the rough coordinates of strip, calculating the normal vectors of the rough coordinates and the accurate coordinates.

Extraction of Rough Coordinates. In order to extract the centerline rough coordinates, the region of interest (ROI) should be extracted firstly. The grayscale distribution of the laser stripe image modulated by the amplitude of web vibration is very obvious,

which is divided into two parts: laser stripe (foreground) and web (background). As the high energy characteristic of the laser stripe, its gray value is mostly distributed near the high value. On the contrary, the web is in the dark environment and its gray value is distributed near low value. Therefore, a suitable threshold T needs to be found to separate the foreground and background. Adaptive threshold segmentation called Otus's method [12] is used in this paper to achieve this threshold T.

The ratio of the laser stripe pixels to the image is μ_0 and the average gray value of the laser stripe is ω_0. The ratio of the web pixels to the image is μ_1 and the average gray value of the web is ω_1. The average gray value of the whole image is μ. So, the variance g between the laser stripe and the web is given as $g = \omega_0(\mu_0 - \mu)^2/(1 - \omega_0)$. Therefore, the best threshold T for separating the laser stripe and the web is the threshold which makes the variance g reaches the maximum.

Since ROI has been found, the rough coordinates of centerline can be obtained next step. Considering that the noise is small in the ROI of laser stripe, and the amplitude of the web vibration is also small which means that the amount of the laser stripe deformation is small, gray centroid method is utilized to achieve the rough coordinates.

In the ROI of the stripe, (x_m, y_i) is used to denote the coordinates of the m column in the stripe section and the corresponding gray value is $I(x_m, y_i)(i = 1, 2, \ldots, N)$. N is used to denote the number of points in the stripe section, which is usually taken as an odd number. Then, the column coordinate y_m is given as

$$y_m = \sum_{i=1}^{N} I(x_m, y_i) \cdot y_i / \sum_{i=1}^{N} I(x_m, y_i) \tag{5}$$

The results obtained by the Eq. (5) are shown in Fig. 2.

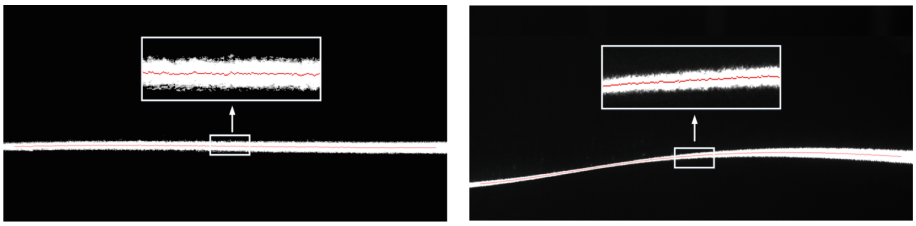

(a) (b)

Fig. 2. The rough coordinates obtained by gray centroid method (a) linear laser stripe; (b) curvilinear laser stripe.

Extraction of Normal Vectors. In this section, the method for obtaining the normal vectors of laser strip will be discussed. In order to obtain the normal vectors, gray images need to be converted from gray space to the gradient vector space. $I(x, y)$ is used to denote the gray value of the rough point $P(x, y)$. Then using the Sobel operator, the gradient vector at point P is given as

$$[G_x, G_y]^T = [\frac{\partial I(x,y)}{\partial x}, \frac{\partial I(x,y)}{\partial y}]^T \tag{6}$$

Next, v is used to denote the unit normal vector at the point P. The sum of the projection of gradient vector dataset on the unit normal vector v can be defined as

$$G^T v = \frac{1}{N}\sum_{i=1}^{N}(G^{i^T} \cdot v) = v^T(\frac{1}{N}\sum_{i=1}^{N} G^i \cdot G^{i^T})v \tag{7}$$

in a window W. Since v is a unit normal vector, solving the maximum value of the formula (7) is to obtain the main eigenvector of the auto covariance matrix C, i.e.,

$$\begin{aligned} C &= \begin{bmatrix} Cov(G_x, G_x) & Cov(G_x, G_y) \\ Cov(G_y, G_x) & Cov(G_y, G_y) \end{bmatrix} \\ &= \begin{bmatrix} E[G_x^2] - (E[G_x])^2 & E[G_xG_y] - E[G_x]E[G_y] \\ E[G_xG_y] - E[G_x]E[G_y] & E[G_y^2] - (E[G_y])^2 \end{bmatrix} \end{aligned} \tag{8}$$

In this estimate of the auto covariance matrix C, the assumption is made that the gradient vectors are zero-mean, i.e., $E[G_x] = E[G_y] = 0$, in the window W. Therefore, the eigenvalues and eigenvectors of the auto covariance matrix are derived as

$$\begin{aligned} \lambda_1 &= \frac{E[G_x^2] + E[G_y^2]}{2} + \frac{\sqrt{(E[G_x^2] - E[G_y^2])^2 + 4E[G_xG_y]^2}}{2} \\ \lambda_2 &= \frac{E[G_x^2] + E[G_y^2]}{2} - \frac{\sqrt{(E[G_x^2] - E[G_y^2])^2 + 4E[G_xG_y]^2}}{2} \\ v_1 &= \left[\frac{E[G_x^2] - E[G_y^2]}{2} + \frac{\sqrt{(E[G_x^2] - E[G_y^2])^2 + 4E[G_xG_y]^2}}{2} \quad E[G_xG_y]\right]^T \\ v_2 &= \left[\frac{E[G_x^2] - E[G_y^2]}{2} - \frac{\sqrt{(E[G_x^2] - E[G_y^2])^2 + 4E[G_xG_y]^2}}{2} \quad E[G_xG_y]\right]^T \end{aligned} \tag{9}$$

By the definition of the gradient vectors auto covariance matrix, the eigenvector corresponding to the maximum absolute value of the eigenvalues is the normal vector of stripe. The results obtained by the Eq. (9) are shown in Fig. 3.

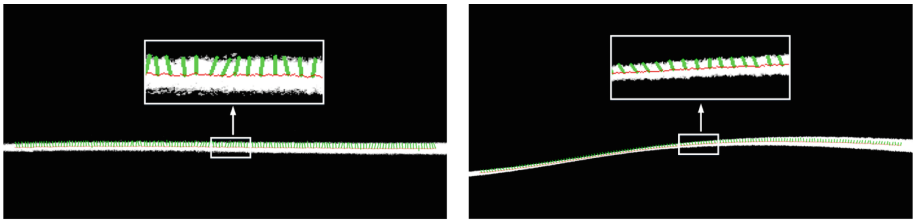

(a) (b)

Fig. 3. The normal vectors obtained based on principal component analysis (a) linear laser stripe; (b) curvilinear laser stripe.

Finally, along the normal direction of each rough coordinate, the accurate coordinate of point $P(x_a, y_a)$ can be given as

$$x_a = \begin{cases} \dfrac{\sum_{i=-W/2}^{i=W/2} I(x_0+i, y_0+ki)\cdot(x_0+i)}{\sum_{i=-W/2}^{i=W/2} I(x_0+i, y_0+ki)}, \theta \in (-\frac{\pi}{2}, -\frac{\pi}{4}] \cup [\frac{\pi}{4}, \frac{\pi}{2}) \\ \dfrac{\sum_{i=-W/2}^{i=W/2} I(x_0-\frac{1}{k}i, y_0+i)\cdot(x_0-\frac{1}{k}i)}{\sum_{i=-W/2}^{i=W/2} I(x_0-\frac{1}{k}i, y_0+i)}, \theta \in (-\frac{\pi}{4}, \frac{\pi}{4}) \end{cases}$$

$$y_a = \begin{cases} \dfrac{\sum_{i=-W/2}^{i=W/2} I(x_0+i, y_0+ki)\cdot(y_0+ki)}{\sum_{i=-W/2}^{i=W/2} I(x_0+i, y_0+ki)}, \theta \in (-\frac{\pi}{2}, -\frac{\pi}{4}] \cup [\frac{\pi}{4}, \frac{\pi}{2}) \\ \dfrac{\sum_{i=-W/2}^{i=W/2} I(x_0-\frac{1}{k}i, y_0+i)\cdot(y_0+i)}{\sum_{i=-W/2}^{i=W/2} I(x_0-\frac{1}{k}i, y_0+i)}, \theta \in (-\frac{\pi}{4}, \frac{\pi}{4}) \end{cases} \tag{10}$$

where k denotes the normal slope at the rough coordinate of the stripe and θ denotes the tilt angle of normal slope at the rough coordinate. The results obtained by the Eq. (10) are shown in Fig. 4.

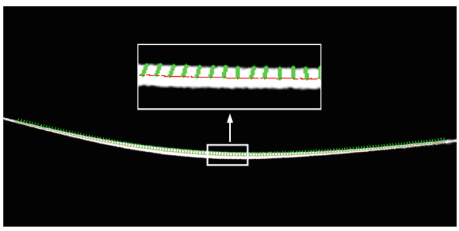

Fig. 4. The accurate coordinates of centerline laser stripe.

4 Experiments

The experiments are performed on a R2R system, as shown in Fig. 5. The CCD camera is vertical to the web surface to measure the out-of-plane displacements, which has a sampling frequency of 50 Hz. The data acquisition, A/D conversion and data processing are all carried out using the Universal Motion and Automation Controller (UMAC) and Visual Studio 2015 software. The UMAC is a systemic controller of Delta Tau. The experimental results are compared with the vibration frequencies derived from the string model.

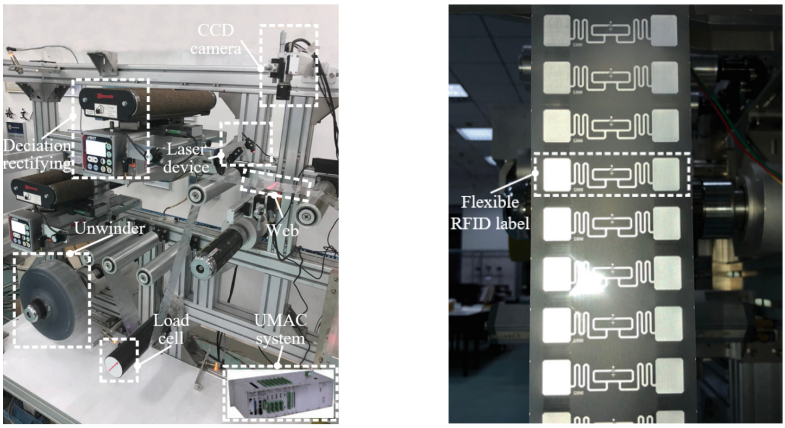

Fig. 5. The R2R experimental environment (a) The R2R platform; (b) The web used in experiments.

The RFID inlay (see in Fig. 5(b)), one PET substrate with patterning antenna, is used as the travelling web in this experiment. The dimensions of the web are $L = 0.380\,\text{m}$, $b = 0.084\,\text{m}$, $h = 5 \times 10^{-5}\,\text{m}$, $\rho = 0.0580\,\text{kg/m}^3$. Because of large amount of experimental data, three feature points in the web are selected at the same interval to explain. The natural frequencies in different states calculated by the string model is shown in Table 1.

Table 1. The natural frequencies of the RFID inlay in different states.

Tension (N)	Stationary web f_1 (HZ)	Moving web (V = 10) f_2 (HZ)	Moving web (V = 20) f_3 (HZ)
4	10.927	10.923	10.909
6	13.383	13.378	13.361
8	15.453	15.447	15.428
10	17.277	17.270	17.249

4.1 Static Experiments

For the stationary web, the tension is set 4 N. From the centerline extraction algorithm proposed in this paper, the vibration displacements are calculated. From the Fourier transform, the natural frequencies are also calculated in the range from 0 Hz to 30 Hz. The displacement-time curves and amplitude-frequency diagram are shown in Fig. 6. It is seen that the detected first natural vibration frequencies of the three points are 11.52 Hz, 10.55 Hz, 11.23 Hz, respectively. The experimental results show good agreement with the theoretical results predicted with the simple string model.

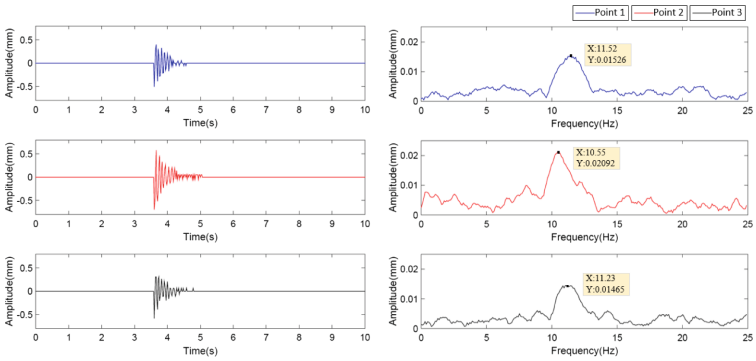

Fig. 6. The displacement-time curve are amplitude-frequency curve for the stationary web when $T = 4$ N.

4.2 Dynamic Experiments

For the web in dynamic state, the effect of the travelling speed on the natural frequencies should be taken into consideration [13, 14]. The web tension is set 4 N while the web velocity is set 10 m/min and the web tension is set 6 N while the web velocity is set 20 m/min. The displacement-time curves and amplitude-frequency diagram are shown in Figs. 7 and 8, respectively.

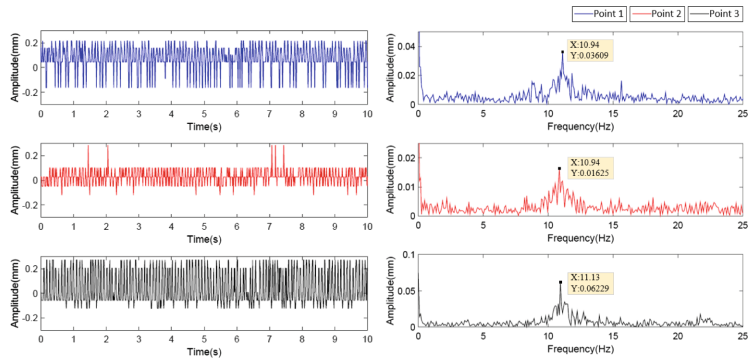

Fig. 7. The displacement-time curve are amplitude-frequency curve for the web when $T = 4$ N and $V = 10$ m/min.

The comparisons of the web vibration frequencies estimated by the proposed method and the string model are shown in Table 2. As a result, the frequencies of the different position are close to the frequencies calculated by the string model. The error of the web vibration frequency estimated by the proposed method is within 6%. The proposed method based on the vision technique can conveniently measure the web vibration distribution. It is noted that, for the web vibration measurement, discrepancies of results may be caused by following reasons: (a) the fitting error in the structured light stereovision geometrical model; (b) the material parameters of web; (c) the resolution of measured amplitudes using CCD camera.

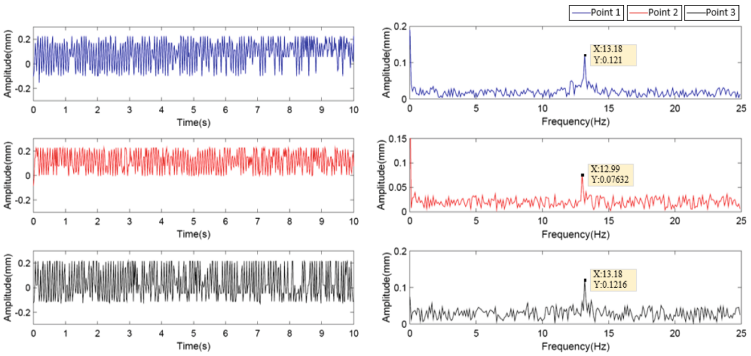

Fig. 8. The displacement-time curve are amplitude-frequency curve for the web when $T = 6$ N and $V = 20$ m/min.

Table 2. The comparison of the web vibration frequency estimated by the proposed method and the frequency by the string model.

Web speed V (m/min)	Tension T (N)	Point	Measured frequency f_m (Hz)	Theoretical frequency f_t (Hz)	Error $\lvert f_m - f_t \rvert / f_t$
0	4	1	11.52	10.927	5.42%
		2	10.55	10.927	3.45%
		3	11.23	10.927	2.77%
10	4	1	10.94	10.923	0.16%
		2	10.94	10.923	0.16%
		3	11.13	10.923	1.90%
20	6	1	13.18	13.361	1.35%
		2	12.99	13.361	2.78%
		3	13.18	13.361	1.35%

5 Conclusions

In this paper, we have presented a new measurement technique for the out-of-plane vibration distribution of a moving web. A structured light stereovision geometrical model is used to achieve the precise amplitudes of web vibration. Also, the centerline extraction of laser stripe based on the principal component analysis is proposed. The vibration frequencies distributed along the stripe is successfully estimated and the error is generally less than 6%. The main advantage of this measurement is its non-contact with web, which has no additional influence on the moving web. Also, there is no need to change or modify the existing layout of the web handling machine.

References

1. Rogers, J., Someya, T., Huang, Y.: Materials and mechanics for stretchable electronics. Science **327**, 1603–1607 (2010)
2. Ma, L., Chen, J., Tang, W., Yin, Z.: Vibration-based estimation of tension for an axially travelling web in roll-to-roll manufacturing. Measur. Sci. Technol. **29**, 015102 (2018)
3. Guo, J., Zheng, Z., Wu, S.: An impact vibration experimental research on the pretension rectangular membrane structure. Adv. Mater. Sci. Eng. **2015**, 1–8 (2015)
4. Prakash, S., Upadhyay, S., Shakher, C.: Real time out-of-plane vibration measurement/monitoring using Talbot interferometry. Optics Lasers Eng. **33**, 251–259 (2000)
5. Maurice, X., Graebling, P., Doignon, C.: A pattern framework driven by the hamming distance for structured light-based reconstruction with a single image. In: Computer Vision and Pattern Recognition, pp. 2497–2504 (2011)
6. Ishii, I., Takemoto, S., Takaki, T., et al.: Real-time laryngoscopic measurements of vocal-fold vibrations. In: International Conference of the IEEE Engineering in Medicine & Biology Society, p. 6623 (2011)
7. Zhai, S.L.: Vibration mode analysis of membrane based on bi-color fringe projection. Optics Optoelectron. Technol. **2**, 015 (2013)
8. Doignon, C., Knittel, D.: A structured light vision system for out-of-plane vibration frequencies location of a moving web. Mach. Vis. Appl. **16**, 289 (2005)
9. Doignon, C., Knittel, D., Maurice, X.: A vision-based technique for edge displacement and vibration estimations of a moving flexible web. IEEE Trans. Instr. Measur. **57**, 1605–1613 (2008)
10. Shin, C., Kim, W., Chung, J.: Free in-plane vibration of an axially moving membrane. J. Sound Vibr. **272**, 137–154 (2004)
11. Vedrines, M., Gassmann, V., Knittel, D.: Moving web-tension determination by out-of-plane vibration measurements Using a Laser. IEEE Trans. Instr. Measur. **58**(1), 207–213 (2009)
12. Otsu, N.: A threshold selection method from gray-level histograms. IEEE Trans. Syst. Man Cybern. **9**(1), 62–66 (1979)
13. Jaberzadeh, E., Azhari, M., Boroomand, B.: Free vibration of moving laminated composite plates with and without skew roller using the element-free Galerkin method. Iran. J. Sci. Technol. Trans. Civ. Eng. **38**, 377–393 (2014)
14. Tang, Y.Q., Chen, L.Q., Zhang, H.J., Yang, S.P.: Stability of axially accelerating viscoelastic Timoshenko beams: recognition of longitudinally varying tensions. Mech. Mach. Theor. **62**, 31–50 (2013)